Refined BCF-type boundary conditions for mesoscale surface step dynamics

Renjie Zhao,[1,2] David M. Ackerman,[1] and James W. Evans[1,2,3]
[1]*Ames Laboratory–USDOE, Iowa State University, Ames, Iowa 50011, USA*
[2]*Department of Physics and Astronomy, Iowa State University, Ames, Iowa 50011, USA*
[3]*Department of Mathematics, Iowa State University, Ames, Iowa 50011*
(Received 16 April 2015; published 24 June 2015)

Deposition on a vicinal surface with alternating rough and smooth steps is described by a solid-on-solid model with anisotropic interactions. Kinetic Monte Carlo (KMC) simulations of the model reveal step pairing in the absence of any additional step attachment barriers. We explore the description of this behavior within an analytic Burton-Cabrera-Frank (BCF)-type step dynamics treatment. Without attachment barriers, conventional kinetic coefficients for the rough and smooth steps are identical, as are the predicted step velocities for a vicinal surface with equal terrace widths. However, we determine refined kinetic coefficients from a two-dimensional discrete deposition-diffusion equation formalism which accounts for step structure. These coefficients are generally higher for rough steps than for smooth steps, reflecting a higher propensity for capture of diffusing terrace adatoms due to a higher kink density. Such refined coefficients also depend on the local environment of the step and can even become negative (corresponding to net detachment despite an excess adatom density) for a smooth step in close proximity to a rough step. Our key observation is that incorporation of these refined kinetic coefficients into a BCF-type step dynamics treatment recovers quantitatively the mesoscale step-pairing behavior observed in the KMC simulations.

DOI: 10.1103/PhysRevB.91.235441 PACS number(s): 68.55.J−, 68.35.Fx, 68.35.bg, 05.10.Ln

I. INTRODUCTION

The evolution of crystalline surface morphologies with a well-defined terrace-step structure and mesoscale terrace widths (from ∼10 to ∼100 nm) is naturally described within a Burton-Cabrera-Frank (BCF)-type step dynamics treatment [1–3]. Such treatments utilize suitable evolution laws to track the motion of the step edges described by continuous curves. In principle, this approach is more efficient than tracking the motion of all surface atoms in stochastic lattice-gas modeling, and is more appropriate than a formulation in terms of a continuum height function which neglects vertical discreteness [4,5]. To describe surface evolution during deposition in the BCF treatment, one solves a simple deposition-diffusion equation on each terrace with suitable boundary conditions (BCs) to determine the flux of diffusing terrace adatoms attaching to or detaching from the steps. This analysis, together with an accounting of possible contribution from step edge diffusion, allows determination of step velocities. This in turn enables propagation of step positions and thus of surface morphology with either Lagrangian front tracking methods [6] or with Eulerian level-set methods [7].

However, there remain some significant obstacles to effective implementation of a precise step dynamics treatment of film growth, in contrast to atomistic models which can be precisely analyzed by kinetic Monte Carlo (KMC) simulation [4,5]. First, there exist mainly heuristic formulations of the kinetic coefficients which appear in the Chernov-type BCs [8] for the deposition-diffusion equation. There is evidence that these heuristic BCs are inadequate to describe evolution on the mesoscale where characteristic lengths for the surface morphology such as terrace widths are not significantly greater than intrinsic lengths such as the mean separation of kinks on step edges [9]. This mean kink separation becomes large on straight quasifacetted steps. These limitations are evident in analysis of both surface evolution during deposition [9] and post-deposition coarsening processes [10]. There exist some recent theoretical developments for more systematic determination of kinetic coefficients from atomistic models. These either utilize a kinetic model for step edge structure and dynamics (with edge atom and kink densities analyzed at the mean-field level in a nonequilibrium steady state) [11], or employ discrete two-dimensional (2D) deposition-diffusion equations (DDEs) where some details of step structure, i.e., kink distributions, can be incorporated [9]. Another issue (which we do not address in this study) is the lack of a rigorous formulation for step edge diffusion fluxes in far-from-equilibrium growth situations, in contrast to the Mullin's type formulation for near equilibrium regime [3,5].

Our focus in this study is on step flow during deposition on so-called AB-vicinal surfaces which are characterized by alternating step types. This feature naturally occurs for vicinal surfaces of hexagonal close packed (hcp) metal crystals, and for reconstructed Si(100) and Ge(100) surfaces. The specific solid-on-solid (SOS) lattice-gas model considered here [9,12] was motivated by the latter semiconductor systems, and exhibits alternating rough and smooth steps with no additional barrier for step attachment. KMC simulations reveal step pairing where rougher steps initially advance faster than smoother steps. In contrast, a BCF-type treatment of this system using conventional kinetic coefficients in the Chernov BCs fails to capture this feature. Thus, we will implement a refined BCF-type treatment in an attempt to correct for this failure.

Specifically, in this study, we utilize the previous development in Ref. [9] of a basic discrete 2D DDE formalism to determine kinetic coefficients for a specific fixed step geometry on a vicinal surface. However, going beyond Ref. [9], the current work:

(i) extends the approach in [9] via an iterative analysis to treat evolving stepped surface morphologies, and applies the approach to describe step pairing on AB-vicinal surfaces;

(ii) validates the 2D DDE formalism by detailed comparison against precise predictions for step pairing from KMC simulation of a suitable anisotropic solid-on-solid model;

(iii) extends the basic formalism of [9] beyond simple periodic distributions of kinks along steps to better describe actual stochastic kink distributions;

(iv) demonstrates the importance at least for narrower terraces of "direct deposition" at step edges (versus terrace diffusion to steps) in impacting step velocities;

(v) reveals that the increase of kinetic coefficients with increasing kink density and thus step roughness is key for step pairing where rough steps catch up to smooth steps;

(vi) reveals that not only do kinetic coefficients depend on the local environment of a step, but that they can become negative (corresponding to net detachment from a step even with excess local adatom density) for a smooth step close to a rough step.

Section II provides a brief description of the atomistic lattice-gas model and KMC simulation results. In Sec. III we first describe the BCF-type step dynamics treatment with conventional kinetic coefficients. Then we present the 2D discrete DDE formalism from which refined coefficients can be obtained which account for step structure. Results for and discussion of the behavior of these coefficients are also provided. Section IV compares results from KMC simulation and our refined BCF (rBCF) treatment for step dynamics and specifically step pairing. Section V provides conclusions.

II. ATOMISTIC SOS MODEL FOR STEP FLOW ON AN AB-VICINAL SURFACE

The basic SOS lattice-gas model for deposition on a vicinal surface considered here was initially developed and explored in Ref. [12]. First, we describe the surface structure and energetics incorporated into the model, which control *equilibrium properties* (behavior which is revealed in the absence of deposition). Below, T denotes the surface temperature, k_B the Boltzmann constant, and $\beta = 1/(k_B T)$ the inverse temperature. SOS models adopt a simple-cubic crystalline lattice structure, where the lattice constant a is often set to unity for convenience. For the vicinal surface geometry of relevance here, the steps are aligned with a principal lattice direction and one adopts appropriate skewed periodic boundary conditions for the simulation cell. The model considered here also includes *anisotropic* lateral nearest-neighbor (NN) interactions between atoms with strong attractions, $\phi_S > 0$, and weak attractions, $\phi_W > 0$, in orthogonal directions. Also, significantly, the direction of the strong (and weak) interactions *alternates* between adjacent layers or terraces of the vicinal surface.

Thus, if on one terrace, the strong interaction is aligned with the direction of the steps (a principal lattice direction), then on the adjacent terraces the weak interaction will be aligned with the step direction. In the former case, the energy cost to create a kink at the ascending step bordering the terrace will be $\varepsilon_S = \phi_S/2$, since one strong bond is broken upon separating one contiguous string of atoms at a step edge into two strings (which creates two kinks facing in opposite directions). On the adjacent terraces, the kink creation energy at the ascending steps will be $\varepsilon_W = \phi_W/2$. Through a Boltzmann analysis neglecting multiheight kinks, the equilibrium probability per site p_k of kinks is roughly given in terms of the kink creation energies ε by $p_k \approx 2e^{-\beta\varepsilon}/(1 + 2e^{-\beta\varepsilon})$ [2,13]. Thus, p_k is lower for higher ε, and the model will display alternating rough (r) and smooth (s) steps on adjacent terraces. We set $\beta\phi_S = 6.3$ (and $\beta\phi_W = 3.2$) producing rough estimates for mean kink separations $L_k = a/p_k$ of $L_{ks} \approx 12.7a$ (and $L_{kr} \approx 3.48a$) for smoother (rougher) steps. See Fig. 1(a) for simulated equilibrium configurations for our SOS model, analysis of which yields $L_{ks} \approx 14.2a$ ($L_{kr} \approx 3.69a$) for smoother (rougher) steps close to the above estimates. Despite the difference in step structure, steps of both types are associated with the same equilibrium adatom density $n_{\rm eq} = \exp(-\beta\phi_B)$, where $\phi_B = \phi_S + \phi_W$ is the energy cost to extract an adatom from the kink site to the terrace. The unique $n_{\rm eq}$ follows as the chemical potential of both step types (which are in equilibrium with this adatom density and with each other) must be equal.

Next, we first describe *kinetic aspects* of a general version of the SOS model, before restricting our consideration to a special case. The model includes: (i) deposition at rate F per site; and (ii) thermally activated hopping of surface adatoms to NN empty sites either within the same or adjacent layers with Arrhenius hop rates, $h_\alpha = \nu\exp[-\beta E_{\rm act}(\alpha)]$, where the activation barrier for hopping $E_{\rm act}(\alpha)$ depends on the local environment α. The coverage of deposited material is denoted by $\theta = Ft$ monolayers (ML), where t is the deposition time. In this model, intralayer terrace diffusion of isolated adatoms is *isotropic* with barrier $E_{\rm act} = E_d$, so the hop rate is given by $h = \nu\exp(-\beta E_d)$. For more general hops, the barrier is given by

$$E_{\rm act} = E_d + m_S\,\phi_S + m_W\phi_W + \Delta_\pm\delta_\pm. \qquad (1)$$

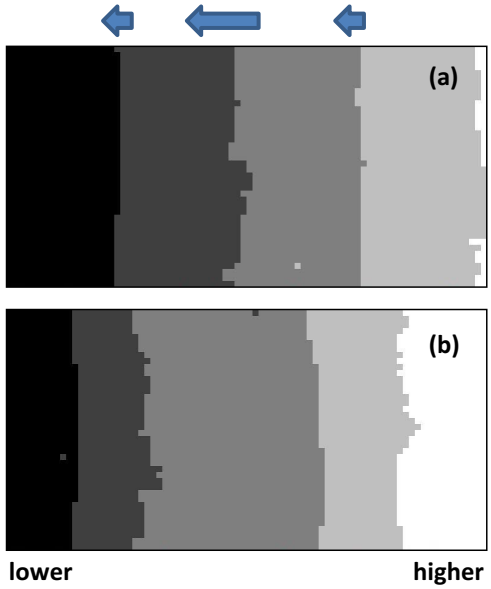

FIG. 1. (Color online) KMC simulation results for step evolution on a vicinal surface ascending to the right in the anisotropic SOS model: (a) initial predeposition geometry with equal mean terrace widths of $20a$ and (b) morphology after deposition of $\sim$0.54 ML. The simulations set $h/F = 10^8$. Image size: $40a \times 80a$.

Here m_S (m_W) is the number of adjacent adatoms in the same layer *before* hopping with a strong (weak) attraction to the hopping adatom. The + (−) sign applies for intra- (inter-) layer hops. Also for intralayer hops, $\Delta_+ = 1$ for hops corresponding to attachment to or detachment from an ascending step, and $\Delta_+ = 0$ otherwise [14]. Also, $\delta_+ \geqslant 0$ represents an additional barrier for attachment to ascending steps, but we will set $\delta_+ = 0$ in our analysis. For interlayer hops up or down monoatomic steps, $\Delta_- = 1$, and δ_- corresponds to the additional Ehrlich-Schwoebel barrier for attachment to descending steps. In our analysis, we will also set $\delta_- = 0$, so that there are no barriers for attachment to either ascending of descending steps. This formulation for environment-dependent activation barriers is often referred to as Clarke-Vvedensky bond counting [15] or the "initial value approximation" (IVA) [16]. The IVA is generally regarded as providing a reasonable description of thermally activated hopping on semiconductor surfaces, but does not effectively capture behavior on metal surfaces [5].

Figure 1 shows typical simulation results for evolution during deposition of the morphology of a vicinal surface ascending from left to right. Figure 1(a) shows the equilibrium surface structure prior to deposition with equal mean terrace widths of $20a$ for the two types of terraces bordered by alternating rough and smooth steps. Deposition results in more rapid initial advance of the rough steps (to the left), resulting in step pairing. See Fig. 1(b). Quantitative results related to this step pairing behavior will be presented in Sec. IV for comparison with results from the refined BCF treatment.

III. REFINED BCF TREATMENT FOR MESOSCALE STEP DYNAMICS

A. BCF treatment with Chernov boundary conditions and refinements

The standard continuum BCF treatment of step flow during deposition is based on quasi-steady-state solutions for the adatom density $\rho(\underline{x},t)$ per unit area at lateral position $\underline{x}$ and time t. This density satisfies the continuum deposition-diffusion equation

$$\partial/\partial t\, \rho(\underline{x},t) = F_c + D\nabla^2\, \rho(\underline{x},t) \approx 0, \qquad (2)$$

where $F_c = a^{-2}F$ denotes the deposition flux per unit area, and $D = a^2 h$ is the terrace diffusion coefficient (again where it is often convenient below to set the lattice constant $a = 1$). General Chernov-type BCs at step edges [8], also accounting for possible step permeability [17], have the form

$$J_\pm = \mp D\nabla_n \rho|_\pm = K_\pm(\rho_\pm - \rho_{\rm eq}) + P(\rho_\pm - \rho_\mp). \qquad (3)$$

Here $\nabla_{\rm n}$ denotes the gradient normal to the step. $J_\pm$ denote the net diffusion fluxes for attachment to an ascending step from the terrace below (+) and to a descending step from above (−), $\rho_\pm$ are the limiting values of the terrace adatom density approaching the step on the lower (+) and upper (−) terrace, $K_\pm$ are the corresponding Chernov kinetic coefficients, P is the step permeability, and $\rho_{\rm eq}$ denotes the equilibrium adatom density at the step. The sign convention is chosen for a vicinal surface ascending to the right and where we define net attachment fluxes to be positive, $J_\pm > 0$. The velocity of the step is given by $V = J_+ + J_- + J_{\rm edge}$, where $J_{\rm edge}$ is the contribution from edge diffusion [5], which vanishes for the straight steps of interest here.

Note that Eq. (3) ignores convection terms associated with the motion of the steps at finite velocity [18,19]. However, these terms are reasonably neglected as steps move very slowly on the time scale of adatom density relaxation. More precisely, these terms can be neglected if the jump in adatom density per site across the step is far below unity. An upper bound on the adatom density per site, and thus on the jump in density, is given by $(F/h)w^2$, where w is the typical terrace width in units of lattice constants. For example, one finds that $(F/h)w^2$ is no higher than $10^{-4.5}$ for the studies of step flow on Si(100) in [12], so that convection terms are completely negligible.

It is instructive to rewrite the kinetic coefficients (which reflect the ease of attachment to steps) as $K_\pm = D/\Gamma_\pm$, where $\Gamma_\pm$ are the attachment lengths (large values of which imply difficult attachment). If the step permeability term is *absent* (as discussed further below), solution of the boundary value problem for the deposition-diffusion equation on a single linear terrace of width W yields [4,5]

$$J_\pm = F_c W\,(1/2 + \Gamma_\mp/W)/(1 + \Gamma_+/W + \Gamma_-/W). \qquad (4)$$

We caution that the + (−) in (4) indicate diffusion fluxes and attachment lengths for *different* ascending (descending) steps at the right (left) edge of the *same* terrace. Note that $J_+ + J_- = F_c W$ by mass conservation.

One significant refinement of the above treatment which will be needed for the success of our subsequent analysis is to account for the feature that the surface lattice constant a need not be insignificant compared to terrace widths W. Within the context of SOS modeling, it is reasonable to assert that atoms depositing directly within a strip of width a of the edge of the ascending step attach directly to that step, i.e., that atomistic effects should be accounted for in the continuum modeling [20]. Then, there exists a *direct deposition* contribution $J_{\rm dd} = aF_c = a^{-1}F$ to the flux of atoms attaching to the step. Also, the step velocity is now given by $V = J_+ + J_- + J_{\rm edge} + J_{\rm dd}$, where for our application again $J_{\rm edge} = 0$, but now the formulas (4) are replaced by

$$J_\pm = F_c(W - a)\,[1/2 + \Gamma_\mp/(W - a)]/[1 + \Gamma_+/(W - a) + \Gamma_-/(W - a)]. \qquad (5)$$

Heuristic formulations for the kinetic coefficients $K = K_\pm$ or attachment lengths $L_\pm$ are often based on analysis of discrete one-dimensional deposition-diffusion equations [4,5,9]. For additional attachment barriers $\delta_\pm$, this analysis reveals that the attachment lengths satisfy $\Gamma_\pm = [\exp(\beta\delta_\pm) - 1]a$. See Ref. [21] for an alternative derivation of this result. In our SOS model without attachment barriers, this conventional formulation consequently shows that $K_\pm = \infty$, which corresponds to imposing a simple Dirichlet BC, $\rho_\pm = \rho_{\rm eq}$ at steps. However, we shall see that in reality for our model of mesoscale step dynamics without step attachment barriers, the kinetic coefficients $K_\pm$ remain finite. In addition, we find that $\rho_+ = \rho_-$ for a single step, so that the permeability term drops out. Consequently, the relation (5) will apply, but with appropriately refined $K_\pm$ or $\Gamma_\pm$.

B. Basic discrete 2D deposition-diffusion equation formalism

Our discrete 2D deposition-diffusion equation (DDE) formalism is constructed to mimic the geometry, energetics, and kinetics of the SOS model for deposition on a vicinal surface with alternating rough and smooth steps. In the simplest scenario, one could consider vicinal surface geometries of the type illustrated in Fig. 2. On each terrace there is a periodic square array or lattice of adsorption sites labeled (i,j) with lattice constant a. Different terraces are separated by steps along which kinks are distributed periodically, where alternating smooth (s) and rough (r) steps have larger and smaller kink separations, respectively. The larger kink separation $L_{ks} = L$ is an integral multiple m of the smaller one $L_{kr} = L/m$, and the surface geometry is constructed where every mth kink on the rough step aligns with a kink on the smooth step. This scenario is shown in Fig. 2 for $m = 2$. The vicinal surface will in general be constructed with larger (smaller) terrace widths $W_+(W_-)$ for terraces bordered by ascending smooth (rough) steps. Thus, the periodic unit cell for this system has the dimension $L \times (W_+ + W_-)$, as illustrated by the tan shaded region in Fig. 2.

At each adsorption site we will specify an adatom density $n(i,j)$ corresponding to the probability that site (i,j) is occupied. To make a connection with the continuum description of Sec. III A formulated in terms of densities per unit area, if the lateral position on the surface corresponds to $\underline{x} = (ia, ja)$, then one has $\rho(\underline{x},t) \approx a^{-2}\, n(i,j)$. Model kinetics, which implicitly incorporates the underlying model energetics, is formulated in terms of evolution equations for the $n(i,j)$. Specifically, the discrete 2D DDE for $n(i,j)$ have the form (see also Ref. [9])

$$\begin{aligned} d/dt\, n(i,j) = {} & F + h_L(i+1,j)n(i+1,j) + h_R(i-1,j)n(i-1,j) \\ & + h_D(i,j+1)n(i,j+1) + h_U(i,j-1)n(i,j-1) \\ & - [h_L(i,j) + h_R(i,j) + h_D(i,j) + h_U(i,j)]n(i,j), \end{aligned} \tag{6}$$

for $0 \leqslant i < L/a$ and $0 \leqslant j < (W_- + W_+)/a$. We have assumed that the flux is sufficiently low that $n(i,j) \ll 1$, since otherwise the deposition term should be modified to take account of the possibility that site (i,j) might already be occupied. For kink sites $(i_k, j_k) = (0,0)$, $(L,0)$, etc., one sets $n(i_k, j_k) = 1$. Here $h_X(i,j)$ denotes the rate of hopping from site (i,j) to a NN site in a direction $X = L$ (left), R (right), D (down), and U (up) in the (i,j) plane. All of the energetics described for the SOS model and the associated IVA rates are incorporated into the specification of the $h_X(i,j)$. Retaining for the present the possibility of attachment barriers to steps, and also allowing the possibility of arbitrary rates for hopping along straight portions of steps, one has the following specifications: $h_X = h$ for an isolated terrace adatom, $h_X = h_{es}(h_{er})$ for an isolated adatom hopping along straight portion of a smooth (rough) steps, $h_X = \exp(-\beta\delta_\pm)h$ to attach to steps including kink sites from the terrace (choosing δ_+ for ascending and δ_- for descending steps), $h_X = \exp(-\beta\phi_W - \beta\delta_\pm)h$ [$h_X = \exp(-\beta\phi_S - \beta\delta_\pm)h$] to detach from step edges to terraces, $h_X = \exp(-\beta\phi_S)h_{es}$ [$h_X = \exp(-\beta\phi_W)h_{er}$] to detach from kinks to step edge sites on smooth [rough] steps, and $h_X = \exp(-\beta\phi_B - \beta\delta_\pm)h$ to detach directly from kinks to terraces. See Fig. 2. To mimic our SOS model, edge diffusion rates h_{es} and h_{er} are chosen in terms of h and the interactions according to the IVA formulation of Sec. II.

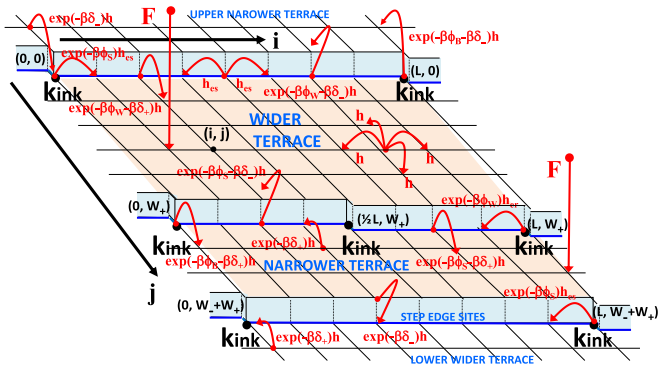

FIG. 2. (Color online) Schematic of the basic discrete 2D deposition-diffusion equation model formulation for a vicinal surface with alternating rough and smooth steps and a ratio $m = 2$ of kink separations on these steps. For convenience we set $a = 1$.

For our application of the above formulation to describe step flow, we need to consider only steady-state behavior of the above discrete 2D DDE. Note that the kink sites constitute both sinks for depositing adatoms and also sources for terrace adatoms. In the absence of deposition ($F = 0$), the steady-state equilibrium density for all terrace sites (i,j) is determined by the density at the kink sites and is given by $n_{\rm eq}(i,j) = \exp(-\beta\phi_B)$, consistent with the SOS model. The equilibrium density for nonkink sites at smooth [rough] step edges is $n_{\rm eq}(i,j) = \exp(-\beta\phi_S)$ [$n_{\rm eq}(i,j) = \exp(-\beta\phi_W)$]. This suggests natural rescaled adatom densities $n^*(i,j)$, where $n^* = n$ for terrace sites, $n^* = \exp(-\beta\phi_W)n$ [$n^* = \exp(-\beta\phi_S)n$] step edge sites at smooth [rough] steps, and $n^* = \exp(-\beta\phi_B)n = \exp(-\beta\phi_B)$ for kink sites. Then, it follows that $n^*_{\rm eq}(i,j) = \exp(-\beta\phi_B)$ for all sites for $F = 0$. Deposition with rate $F > 0$ boosts steady-state $n(i,j)$ or $n^*(i,j)$ above these equilibrium values reflecting a supersaturation of adatom density. Thus, the rescaled excess adatom density satisfies $\delta n^*(i,j) = n^*(i,j) - n^*_{\rm eq}(i,j) > 0$, and this quantity can be shown to be directly proportional to F [9].

C. More general discrete 2D deposition-diffusion equation formalisms

As noted above, in our 2D DDE formalism, one should select the vicinal surface geometry to best match that of the SOS model. Selecting periodic kink distributions, one might anticipate that kink separations should be chosen to match the mean values for the SOS model. In Sec. III B we described the simplest case where the ratio of kink separations on smooth and rough steps was an integer m, in which case the dimension of the periodic unit cell along the steps equals the larger kink separation on the smooth steps. Of course, in the SOS model, typically the ratio of kink separations will not be an integer. Nonetheless, approximating this ratio by a rational number, one can still construct a (larger) periodic unit cell associated with the kink distribution.

However, it is appropriate to critique the above philosophy for selecting kink separations. In the stochastic SOS model,

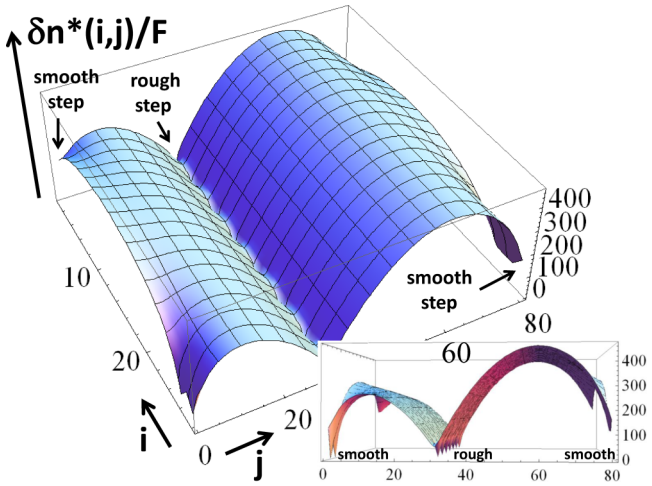

FIG. 3. (Color online) Discrete 2D DDE results for the steady-state excess adatom density $\delta n^*(1,j)/F$ versus $(i,\ j)$ for our SOS model for a vicinal surface with alternating rough and smooth steps. Kink separations are $L_{ks} = 26a$ and $2a$ for smooth steps, and $L_{kr} = 4a$ for rough steps. Alternating narrow and broad terraces have widths $W_- = 30a$ and $W_+ = 50a$, respectively. The inset shows a different 3D perspective of the adatom density variation.

the kinks are not periodically distributed along steps. For smoother steps with low kink density p_{ks}, and large mean separation $L_{ks} = 1/p_{ks}$, the kinks are essentially randomly distributed corresponding to a broad geometric kink separation distribution with standard deviation $\sigma_{ks} \approx L_{ks}$ [13,22]. It is reasonable to expect that for a fixed L_{ks}, a random distribution of kinks which includes a significant number of nearby kink pairs (with separation far below L_{ks}) is *less effective* at capturing diffusing terrace adatoms than a periodic distribution of kinks. This perception will be confirmed in Sec. III D. Thus, we propose that when selecting kink separations in a discrete 2D DDE analysis with simple periodic kink distributions, it would be more appropriate to choose the kink separation to be larger than the mean value in the SOS model. This would better mimic the propensity for adatom capture by the quasirandom distribution of kinks in the SOS model.

Another more sophisticated strategy is to go beyond incorporating simple periodic kink distributions into our discrete 2D DDE. To this end, we could consider the possibility of incorporating biperiodic, triperiodic, etc. kink distributions at least on the smooth step where separations between adjacent kinks cycle between two, three, etc., values, respectively. Note that these choices allow one to retain a periodic unit cell for the discrete 2D DDE analysis. With such distributions, one can match not just the mean kink separation L_{ks} in the SOS model, but also mimic other features of the kink separation distribution. For example, for a biperiodic kink distribution on smooth steps with separations $L_{ks\pm}$, one selects $L_{ks+} = 2L_{ks} - \delta L$ and $L_{ks-} = \delta L$ with $\delta L \ll L_{ks}$, which both matches the mean kink separation $\frac{1}{2}(L_{ks+} + L_{ks-}) = L_{ks}$, and also mimics the large standard deviation $\sigma_{ks} \approx L_{ks}$ of the kink separation distribution. To explicitly illustrate the results of such an analysis, we chose a biperiodic kink distribution with $L_{ks+} = 26a$ and $L_{ks-} = 2a$ for the smooth step. Thus, $L_{ks} = 14a$ is close to our SOS model value. For the rough step we choose $L_{kr} = 4a$ just above the SOS value. Figure 3 shows typical results for the corresponding steady-state excess density $\delta n^*(i,j)$ on a vicinal surface where the structure of the alternating rough and smooth steps is as described above, and where we choose terrace widths of $W_- = 30a$ and $W_+ = 50a$ below the rough and smooth steps, respectively. Naturally $\delta n^*(i,j)$ has a global maximum on each terrace around the middle of the terrace far away from kink site sinks, but also a local maxima along step edges in between kink sites. Also $\delta n^*(i,j)$ smoothly approaches the same value at the step edge from both sides (so that $\rho_+ = \rho_-$ in the notation of Sec. II), and $\delta n^*(i,j)$ also smoothly approaches $\delta n^* = 0$ at kink sites. Of course one could consider even more complex kink distributions better reflecting that in the SOS model, e.g., a biperiodic distribution on the rough step as well as the smooth step, but this has little effect on behavior for our model [23].

D. Kinetic coefficients from the discrete deposition-diffusion equations

Extraction of kinetic coefficients from the discrete 2D DDE model is designed to mimic the continuum BCF treatment, where $K_\pm = J_\pm/(\rho_\pm - \rho_{\rm eq})$ when $\rho_+ = \rho_-$ (or for $P = 0$) from (3). To this end we employ an average ($\langle\rangle$) of key quantities along the step edge. First, we obtain the averaged net attachment fluxes $\langle J_\pm\rangle$ which correspond to the net transfer of atoms from the rows of sites adjacent to the step edge to the row of sites constituting the step edge. Second, we determine the averaged excess adatom density $\langle\delta n^*\rangle$ averaging along the row of sites constituting the step edge. Then, the refined kinetic coefficients are given by $K_\pm = a^2\langle J_\pm\rangle/\langle\delta n^*\rangle$. See Ref. [9] for a more detailed description of this procedure. Since both $\langle J_\pm\rangle$ and $\langle\delta n^*\rangle$ are directly proportional to F, the ratio is independent of F. We note that this formulation for kinetic coefficients is consistent with a determination of step velocities incorporating direct deposition at step edges, corresponding to (5) in Sec. III A, where $V = \langle J_+\rangle + \langle J_-\rangle + J_{\rm dd}$ and $J_{\rm dd} = aF_c = a^{-1}F$.

We briefly mention a few basic and general features of these refined $K_\pm$.

(i) Finite values of $K_\pm < \infty$ follow even in the absence of additional barriers for step attachment since $\langle\delta n^*\rangle > 0$, which in turn reflects the feature that incorporation of diffusing adatoms at steps actually requires diffusion to and attachment at kink sites.

(ii) More detailed analysis for periodic distributions of kinks along steps shows that $K_\pm \sim c/(L_k)^2$, where L_k is the corresponding kink separation.

(iii) More generally, $K_\pm$ depends not just on the density of kinks on the step, but also on the spatial distribution of those kinks.

(iv) Furthermore, $K_\pm$ depends not just on the structure of the step under consideration, but also on the local environment of that step including the widths of nearby terraces (i.e., the distance to nearby steps) and on the nature of nearby steps.

Next, we comment in more detail on the behavior of $K_\pm$ for a biperiodic versus periodic kink distributions on the smooth step in the special case where all terraces have equal width

TABLE I. Kinetic coefficients for a biperiodic distribution of kinks on the smooth step with various separations $L_{ks\pm}$, but fixed $L_{ks} = {}^1\!/_2(L_{ks+} + L_{ks-}) = 14a$ and $L_{kr} = 4a$ for a single terrace width of $W = 20a$. The corresponding ratio of the rough and smooth step velocities is also shown. Note that the reciprocal of aK/D gives the dimensionless attachment length Γ/a. The right column corresponds to Fig. 3.

$L_{ks+}/a, L_{ks-}/a$	14, 14	18, 10	22, 6	24, 4	25, 3	26, 2
aK_s/D	0.0862	0.0826	0.0718	0.0635	0.0583	0.0520
aK_r/D	0.6373	0.6375	0.6381	0.6387	0.6390	0.6395
Velocity ratio	1.84	1.88	2.03	2.18	2.29	2.46

which implies that $K_+ = K_-$ for the same step. Specifically, we compare behavior for a range of choices with fixed $L_{ks} = {}^1\!/_2(L_{ks+} + L_{ks-}) = 14a$ with the benchmark periodic case where $L_{ks+} = L_{ks-} = 14a$. We also set $L_{kr} = 4a$ so that this family of parameters includes that chosen in Fig. 3 as a special case. Results shown in Table I reveal the expected trend already suggested in Sec. III C where the kinetic coefficient for the smooth step K_s decreases from the benchmark periodic case upon making L_{ks-} smaller and L_{ks+} larger. This indicates that adatom capture is less efficient when kinks are clumped together rather than periodically distributed. The kinetic coefficient K_r for the rough step with $L_{kr} = 4a$ is relatively unchanged.

Finally, we provide a more complete analysis of the variation of the kinetic coefficients during step flow (specifically, step pairing) during deposition choosing kink separations $L_{ks+} = 26a$ and $L_{ks-} = 2a$ on the smooth step, and $L_{kr} = 4a$ on the rough step. This matches the choice of parameters selected in Fig. 3. In the following, W_1 denotes the mean width for the terrace below ascending a rough step, and W_2 the mean width for the terrace below smooth steps. Prior to deposition, one has $W_1 = W_2$ for which kinetic coefficients are given in the right column of Table I. After the onset of deposition and step flow, we will find that $W_1 < W_2$, where the sum $W_1 + W_2$ remains constant. For the current study, the key requirement is to "iteratively" assess the kinetic coefficients for each of the rough and smooth steps as a function of the varying terrace widths. We will denote the averaged fluxes to the steps bordering the narrower (wider) terrace by $\langle J_{1\pm}\rangle$ ($\langle J_{2\pm}\rangle$) as indicated in Fig. 4, where $W_1 + W_2 = 80a$. A graphical representation elucidating associated behavior comes first determining the excess adatom density averaged along the terrace $\delta n^*(j) = \sum_i \delta n^*(i,j)/\sum_i 1$ (summing over a unit cell), and then plotting the variation of $\delta n^*(j)$ across the terrace, i.e., versus j.

The averaged profile $\delta n^*(j)$ versus j corresponding to the 3D adatom density plot in Fig. 3 for a vicinal surface with $W_1 = 30a$ and $W_2 = 50a$ is shown in Fig. 4(a). In this case, it is clear that all of $\langle J_{1\pm}\rangle > 0$ and $\langle J_{2\pm}\rangle > 0$, and that $\langle \delta n^*\rangle > 0$ for both steps, so the corresponding kinetic coefficients satisfy $K_{1\pm} > 0$ and $K_{2\pm} > 0$. Analysis for more unequal terrace widths $W_1 = 17a$ and $W_2 = 63a$, which corresponds to a later stage of surface evolution than the above case, is shown in Fig. 4(b). The key difference is that now $J_{1-} < 0$ has become negative (while the other fluxes remain positive), i.e., there is a net flux of detachment from this smoother step towards the rougher step across the narrower terrace. This novel behavior reflects the feature that the rough step is a "strong sink" for diffusing adatoms in close proximity to the smooth step. Since still $\langle \delta n^*\rangle > 0$ for both steps, $J_{1-} < 0$ also implies that $K_{1-} < 0$. A more extensive analysis shows that J_{1-} and thus K_{1-} change sign from positive to negative as W_1 decreases from $21a$ to $20a$.

To demonstrate that this unusual sign-change behavior is not restricted to the special choice of parameters, we also analyze behavior for $W_1 + W_2 = 40a$ (versus $W_1 + W_2 = 80a$ above), retaining the kink separations $L_{ks+} = 26a$, $L_{ks-} = 2a$, and $L_{kr} = 4a$. In fact, for this case, we provide a complete analysis of the variation of kinetic coefficients with terrace width in Table II. Again we see that K_{1-} changes sign from positive to negative as W_1 decreases in this case from $13a$ to $12a$.

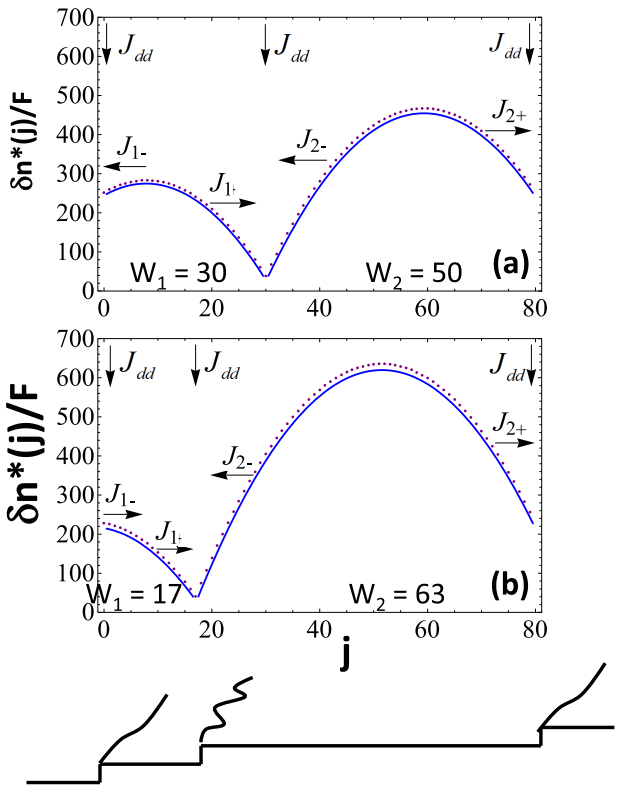

FIG. 4. (Color online) Variation of averaged adatom density profiles across terraces $\delta n^*(j)$ versus j for a vicinal surface with alternating rough and smooth steps: (a) $W_1 = 30a$ and $W_2 = 50a$; (b) $W_1 = 17a$ and $W_2 = 63a$. We set $L_{ks} = 26a$ and $2a$, and $L_{kr} = 4a$. Symbols: Average of 2D DDE results. Curve: 1D continuum DDE results with K's from 2D DDE.

TABLE II. Variation of kinetic coefficients as a function of terrace width where the sum of the mean width of narrower and broader terraces is fixed at $W_1 + W_2 = 40a$. We set $L_{ks} = 26a$ and $2a$, and $L_{kr} = 4a$. The second column indicated the deposited monolayers corresponding to the different terrace widths and follows from our analysis in Sec. IV.

Terrace widths	Deposited monolayers	aK_{1-}/D	aK_{1+}/D	aK_{2-}/D	aK_{2+}/D
20, 20	0	0.052 01	0.639 53	0.639 53	0.052 01
19, 21	0.059 25	0.045 18	0.625 73	0.653 35	0.058 83
18, 22	0.118 37	0.038 30	0.612 05	0.667 08	0.065 69
17, 23	0.177 25	0.031 29	0.598 61	0.680 61	0.072 65
16, 24	0.235 76	0.024 12	0.5855	0.693 84	0.079 78
15, 25	0.293 80	0.016 70	0.572 85	0.706 66	0.087 13
14, 26	0.351 27	0.008 96	0.560 78	0.718 93	0.094 79
13, 27	0.408 08	0.000 80	0.549 42	0.730 53	0.102 85
12, 28	0.464 19	− 0.007 90	0.538 92	0.741 31	0.111 45
11, 29	0.519 57	− 0.017 29	0.529 44	0.751 13	0.120 74
10, 30	0.574 27	− 0.027 59	0.521 14	0.759 81	0.130 93
9, 31	0.628 40	− 0.039 05	0.514 21	0.767 17	0.142 34
8, 32	0.682 25	− 0.052 10	0.508 86	0.773 02	0.155 40
7, 33	0.736 28	− 0.067 28	0.505 29	0.777 14	0.170 73
6, 34	0.791 42	− 0.085 50	0.503 72	0.779 32	0.189 34
5, 35	0.849 36	− 0.108 14	0.504 35	0.779 36	0.212 82
4, 36	0.913 51	− 0.137 63	0.507 30	0.777 09	0.243 99

IV. RESULTS FOR STEP PAIRING: ATOMISTIC MODELING VERSUS REFINED BCF

In an attempt to describe the step pairing observed in the anisotropic SOS model of Sec. II, we utilize a refined BCF (rBCF) analysis of the type described in Sec. III A. We incorporate as input the refined kinetic coefficients determined from analysis of the discrete 2D DDE in Sec. III D with $L_{ks+} = 26a$, $L_{ks-} = 2a$, and $L_{kr} = 4a$. (Again one could input such coefficients for a more complex kink distribution better reflecting that in the SOS model, but we do not expect this to significantly change predicted behavior [23].) In Fig. 5 the results from our rBCF analysis are compared with behavior determined from KMC simulation of the anisotropic SOS model described in Sec. II. For clarity, it is appropriate to describe in more detail the *iterative approach* used in this rBCF analysis. First, at the onset of deposition $t_0 = 0$ where terraces below both step types have equal mean widths, i.e., $W_1 = W_2 = W_0$ (either $20a$ or $40a$ in our simulations), we determine the kinetic coefficients and thus the velocities of the smoother and rougher steps (cf. right column of Table I). From these velocities we estimate the time t_1 and thus the coverage $\theta_1 = Ft_1$, when $W_1 = W_0 - a$ and $W_2 = W_0 + a$. Then we evaluate the kinetic coefficients for these modified terrace widths (cf. Table II), and from them determine the modified velocities of the rougher and smoother steps. From these, in turn, we determine the time t_2 and coverage $\theta_2 = Ft_2$, when $W_1 = W_0 - 2a$ and $W_2 = W_0 + 2a$. Iterating this procedure, we determine from the rBCF analysis the evolution of terrace widths, step velocities, and the step velocity ratio for a sequence of increasing coverages and show by the symbols in Fig. 5.

Predictions from the rBCF analysis (shown as symbols in Fig. 5) are in good agreement with results from KMC simulations of the corresponding SOS model (shown as continuous curves in Fig. 5). For the evolution of the terrace widths, the BCF prediction shows only a slightly greater difference in terrace widths for higher amounts of deposited material around 1 ML. The predictions are also reasonable for more subtle quantities with nontrivial behavior such as step velocities and even the ratio $R_{\rm vel}$ of velocities for rougher and smoother steps. The prediction of the *initial ratio* of step velocities is $R_{\rm vel} = 2.46$ (2.61) from rBCF (KMC) for $W_1 + W_2 = 40a$, and $R_{\rm vel} = 1.77$ (1.74) from rBCF (KMC) for $W_1 + W_2 = 80a$. The lower $R_{\rm vel}$ for wider terraces is expected since the terrace widths are larger in that case compared with the attachment lengths $\Gamma_\pm = D/K_\pm$. Note that as $W_i \to \infty$, one finds that $R_{\rm vel} \to 1$ since attachment at steps becomes limited by diffusion across terraces (irrespective of step structure).

The rBCF treatment also captures the nontrivial behavior of $R_{\rm vel}$ including a slow initial variation before an increase to a maximum, and subsequent decrease towards the asymptotic value of unity. The predicted *maximum* is $R_{\rm vel} = 2.74$ (2.75) from rBCF (KMC) for $W_1 + W_2 = 40a$ occurring at $\theta \approx 0.68$ ($\theta \approx 0.52$) ML, where the ratio of terrace widths equals 4.0 (2.8). The predicted maximum is $R_{\rm vel} = 2.25$ (2.26) from rBCF (KMC) for $W_1 + W_2 = 80a$ occurring at $\theta \approx 1.20$ ($\theta = 1.12$) ML, where the ratio of terrace widths equals 7.0 (5.7). We emphasize that successful recovery of this behavior by the rBCF treatment does not just require significantly different kinetic coefficients for rough and smooth steps. It also requires the feature that kinetic coefficients of a single step differ for upper and lower terraces, and also that they vary in time reflecting the changing local environment of the step.

In support of the above statements and to provide a more detailed elucidation of the behavior of $R_{\rm vel}$, we compare predicted behavior from our rBCF treatment with that of a simpler BCF-type treatment where we allow distinct kinetic coefficients for rough and smooth terraces, but force these to be constant in time. Specifically, we choose these fixed kinetic coefficients to adopt the (initial) values for equal terrace widths, so these take the same value on upper and lower terraces for each type of step (see, e.g., the top row in Table II). Then, analysis of the corresponding vicinal surface evolution shows that $R_{\rm vel}$ decreases

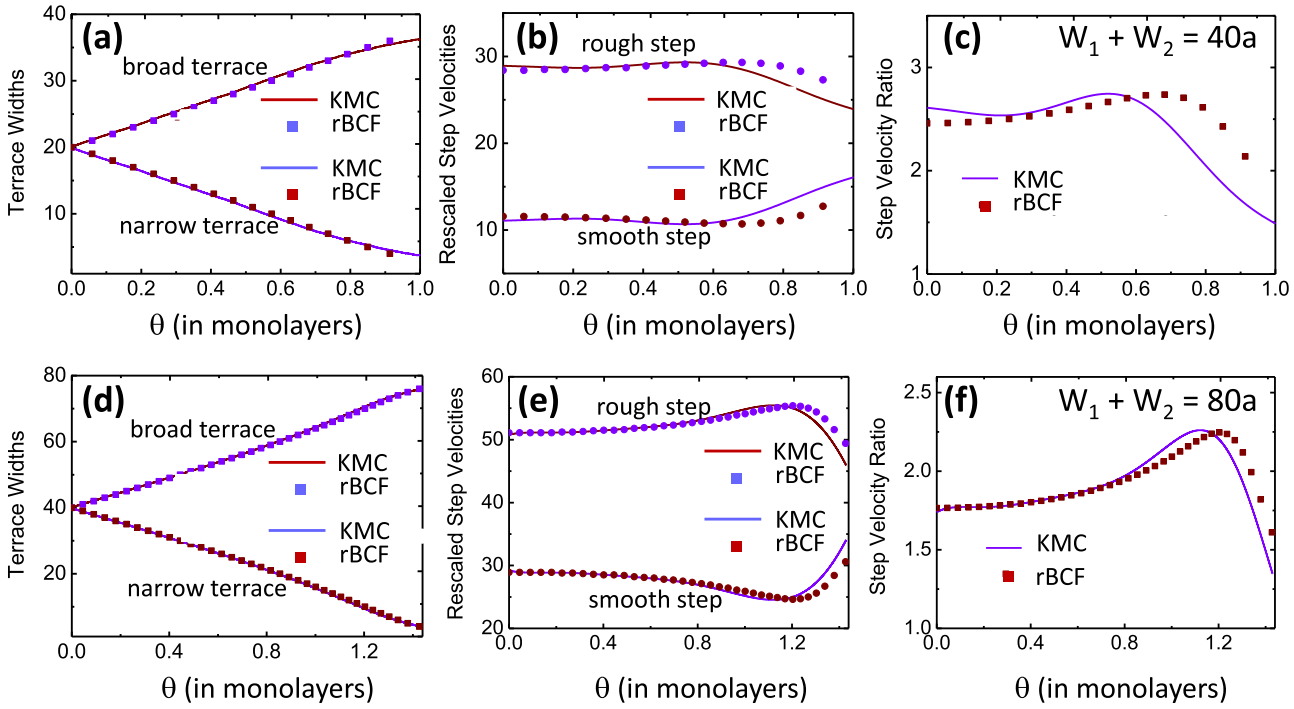

FIG. 5. (Color online) Comparison of rBCF (symbols) and KMC (curves) analysis for step pairing: (a) and (d) terrace widths $W_1 \geqslant W_2$ (in units of a); (b) and (e) rescaled step velocities $V/(aF)$; (c) and (f) step velocity ratio. (a)–(c) $W_1 + W_2 = 40a$; (d)–(f) $W_1 + W_2 = 80a$. We set $L_{ks} = 26a$ and $2a$, and $L_{kr} = 4a$.

monotonically from its initial value rather than exhibiting a local maximum as in the full rBCF treatment (and in the KMC simulations of the SOS model). See Fig. 6. For the simpler BCF-type treatment with constant $K^{'}$s, it is in fact straightforward to show from (4) or (5) that $V_{\rm rel}$ should decrease monotonically to a smaller nonzero value of the point of step collision. The origin of the increase and local maximum in the full rBCF treatment (and in KMC simulations for the SOS model) derives primarily from the feature that the kinetic coefficient for the upper terrace of the smooth step decreases from a small positive value to a significant negative value corresponding to net detachment from this step and enhanced attachment to the nearby trailing rough step. This increases the velocity of the latter.

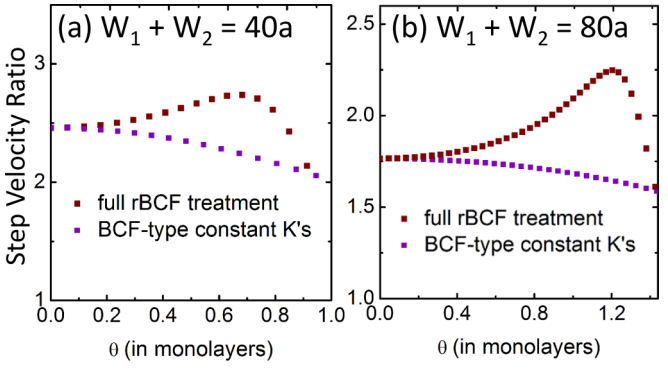

FIG. 6. (Color online) Comparison to step velocity ratio $R_{\rm vel}$ for the full rBCF treatment with a BCF-type treatment incorporating distinct but time-independent $K^{'}$s for rough and smooth steps: (a) $W_1 + W_2 = 40a$; (b) $W_1 + W_2 = 80a$. We set $L_{ks} = 26a$ and $2a$, and $L_{kr} = 4a$.

Finally, we remark that neglecting the role of direct deposition at step edges, i.e., using a treatment based on (4) rather than (5), fails dramatically to recover KMC results for the ratio of step velocities. In fact, in this rBCF treatment, the velocity of the smooth step slows towards zero, so correspondingly $R_{\rm vel}$ grows dramatically. The presence of direct deposition tends to equalize step velocities and avoid this anomalous behavior. See Appendix A for more details. Additional comments on the success and limitations of our rBCF modeling are provided in the conclusions.

V. CONCLUSIONS

Our rBCF treatment has been shown to reliably capture the key features of nontrivial step pairing behavior which was observed in an anisotropic SOS model and precisely quantified by KMC simulation. This SOS model describes a vicinal surface geometry with alternating rough and smooth steps and no additional energetic attachment barriers for either step type. It should be emphasized that a conventional BCF treatment which incorporates infinite kinetic coefficients for both types of steps (which are thus treated as perfect traps) fails to describe the SOS model behavior even qualitatively. In contrast, success of the rBCF treatment requires incorporation of refined kinetic coefficients obtained from the 2D discrete DDE formalism. These coefficients reflect the feature that attachment at step edges in the SOS model requires diffusion-mediated incorporation at kinks, so that the coefficients are finite and decrease (roughly inverse quadratically) with mean kink separation. This feature produces faster initial motion of the rough steps relative to smooth steps, and thus step pairing. Another feature of the refined kinetic coefficients is that they

depend on the local environment, i.e., on the widths of nearby terraces. In fact, kinetic coefficients for the smooth step which is a "weak sink" for diffusing adatoms can become negative (reflecting net detachment) in the presence of a sufficiently close rough step, which is a "strong sink."

The key goal of this paper was a "proof of principle" that a suitably refined BCF treatment can capture subtle step dynamics behavior not described by conventional formulations. Thus, the SOS and rBCF model parameters were selected to clearly display step pairing rather than to describe a specific system. However, it is possible to readily transfer insights from this study to specific systems. For vicinal Si (100), one has that $\varepsilon_S \approx 0.15$ eV and $\varepsilon_W \approx 0.01 - 0.03$ eV [13,24]. With these values one can determine the corresponding mean kink separations $L_k = a/p_k = \frac{1}{2} a e^{+\beta\varepsilon}(1 + 2e^{-\beta\varepsilon})$ for various surface temperatures. The kink separation L_{kr} is effectively always small on rough steps due to the very low ε_W, so these can be regarded as perfect traps with Γ_r well below the terrace width (just as for the rough steps in our modeling). For the smooth steps, one has that $L_{ks} \approx 16a$, for lower growth temperatures around 500 K. Thus, for strongly miscut Si (100) surfaces with narrower terrace widths of $20 - 40a \sim 10 - 20$ nm, the reduced effective kinetic coefficient would produce step pairing similar to that seen in our modeling. One caution is that step equilibration may be inhibited at such lower temperatures, limiting the reliability of the thermodynamic estimate of L_k.

Finally, we remark that although the extent of agreement with KMC simulation results is satisfying, there are limitations to our rBCF treatment. Our rBCF description of step edges involving a periodic or even biperiodic distribution of kink sites is of course an oversimplification to the actual distribution of kink separations and also neglects the presence of multiple height kink at least for rough steps [12]. Another feature which is absent in the rBCF treatment, but present in the SOS model, is effective step-step repulsion. For an actual vicinal surface, repulsion of nearby steps can have entropic or strain origins, but in the SOS model step repulsion is purely entropic. It is possible to modify the rBCF treatment to capture this effect accounting for the feature that entropic repulsion will modify the chemical potential of steps and thus the associated equilibrium adatom density. See Appendix B. However, we have performed selective analyses which indicate that such modifications do not strongly impact step propagation over the range of coverage and step separations considered above.

ACKNOWLEDGMENTS

This work was supported by the U.S. Department of Energy (USDOE), Office of Basic Energy Sciences, Division of Chemical Sciences, Geosciences, and Biosciences through the Ames Laboratory Chemical Physics and CTC programs. The work was performed at Ames Laboratory which is operated for the USDOE by Iowa State University under Contract No. DE-AC02-07CH11358.

APPENDIX A: EFFECT OF DIRECT DEPOSITION AT STEPS

As noted in Sec. IV, it is necessary to implement a rBCF treatment explicitly incorporating direct deposition at step edges in order to even qualitatively capture the behavior of the velocity ratio $R_{\rm vel}$ determined from KMC simulation. To demonstrate this feature, we compare in Fig. 7 the predictions for $R_{\rm vel}$ from rBCF treatments with and without direct deposition at steps (with $L_{ks+} = 26a$, $L_{ks-} = 2a$, and $L_{kr} = 4a$). In the latter case, the dramatic growth in $R_{\rm vel}$ reflects the feature that the smoother step slows towards zero velocity.

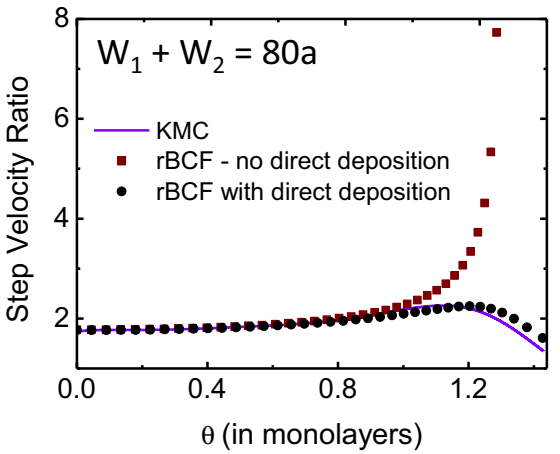

FIG. 7. (Color online) Comparison of rBCF predictions for step velocity ratio with and without direct deposition at step edges. We set $L_{ks} = 26a$ and $2a$, and $L_{kr} = 4a$.

To elucidate the above behavior, we note that the inclusion of direct deposition at step edges is to equalize the step velocities. However, this effect is relatively small so a more complete analysis requires examination of differences in the predicted fluxes $J_{1\pm}$ and $J_{2\pm}$ with and without direct deposition. Figure 8 shows that there is relatively little difference for fluxes on the broad terrace, but a significance difference for fluxes on the narrow terrace. Of most significance is the difference in J_{1-} which is the net detachment flux of atoms from the smooth step across the narrow terrace to the rough step. Significantly higher net detachment rate in the model without direct deposition leads to the above-mentioned dramatic slowing of the smooth step.

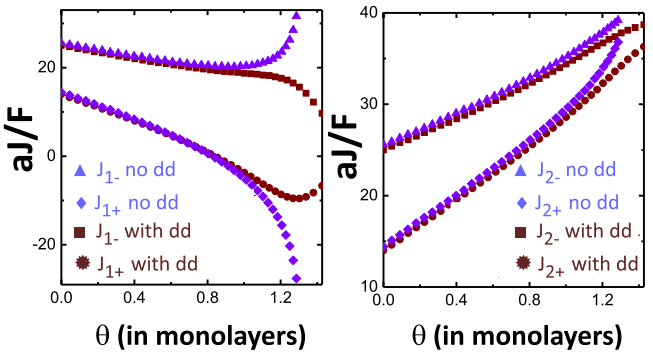

FIG. 8. (Color online) Comparison of rBCF predictions for fluxes with and without direct deposition (dd) at steps. We set $W_1 + W_2 = 80a$, $L_{ks} = 26a$ and $2a$, and $L_{kr} = 4a$.

APPENDIX B: EFFECT OF STEP-STEP REPULSION

The basic effect of step-step repulsion [2] is to increase the chemical potential of the faster moving rougher step as it approaches sufficiently close to the slower moving step (for which the chemical potential is correspondingly reduced). This has the effect of inhibiting attachment to the rougher step and enhancing attachment to the smoother step, thus equalizing the velocities and avoiding step collision. These effects can be incorporated into a BCF or rBCF treatment by appropriately modifying the equilibrium adatom densities at the steps recalling that these densities are directly related to the step chemical potentials.

The connection between the equilibrium adatom density n_{eq} and the step chemical potential μ_{step} is given by $n_{eq} = \exp(\beta\mu_{step})$, where we decompose $\mu_{step} = -\phi_B + \mu_{rep}$. The contribution μ_{rep} represents the effect of step-step repulsion and was neglected in the main text. To quantify this term, we assume that the total step repulsion energy can be written as a sum of pairwise contributions $V(W) > 0$ for each nearest-neighbor pair of steps separated by a terrace of width W. Then, for a specific step with adjacent upper (lower) terrace of width W_U (W_L), it is straightforward to show that $\mu_{rep} = V'(W_L) - V'(W_U)$, where the prime represents the derivative with respect to terrace width [2]. It is believed that $V(W)$ has an inverse square form for entropic repulsion with strength g so that [2,25]

$$V(W) = g/W^2 \quad \text{and} \quad \mu_{rep} = 2g[(W_L)^{-3} - (W_U)^{-3}]. \tag{B1}$$

Applying this result to our system with alternating rough and smooth steps, we find that

$$n_{eq}(\text{rough}) = A_{rep} n^0_{eq} \quad \text{and} \quad n_{eq}(\text{smooth}) = n^0_{eq}/A_{rep}, \tag{B2}$$

where $n^0_{eq} = \exp(-\beta\phi_B)$ and
$A_{rep} = \exp[2\beta g(W_-)^{-3} - 2\beta g(W_+)^{-3}] \geqslant 1$.

The rBCF treatment can be modified to incorporate these different equilibrium adatom densities for different step types. However, we find that for reasonable values of βg, this modification does not significantly change the step dynamics over the range of coverage (and step separations) considered above. For higher coverages (i.e., longer deposition times), such a modification would limit the approach of rough steps towards the smooth steps.

[1] W. K. Burton, N. Cabrera, and F. C. Frank, Philos. Trans. R. Soc. London **243**, 299 (1951).

[2] H.-C. Jeong and E. D. Williams, Surf. Sci. Rep. **34**, 171 (1999).

[3] C. Misbah, O. Pierre-Louis, and Y. Sato, Rev. Mod. Phys. **82**, 981 (2010).

[4] T. Michely and J. Krug, *Islands, Mounds, and Atoms* (Springer, Berlin, 2004).

[5] J. W. Evans, P. A. Thiel, and M. C. Bartelt, Surf. Sci. Rep. **61**, 1 (2006).

[6] G. Dziuk and C. M. Elliot, Acta Numer. **22**, 289 (2013).

[7] C. Ratsch, M. F. Gyure, R. E. Caflisch, F. Gibou, M. Petersen, M. Kang, J. Garcia, and D. D. Vvedensky, Phys. Rev. B **65**, 195403 (2002).

[8] A. A. Chernov, Sov. Phys. Usp. **4**, 116 (1961).

[9] D. M. Ackerman and J. W. Evans, Multiscale Model. Simul. **9**, 59 (2011).

[10] C.-J. Wang, Y. Han, H. Walen, S. M. Russell, P. A. Thiel, and J. W. Evans, Phys. Rev. B **88**, 155434 (2013).

[11] D. Margetis and R. E. Caflisch, Multiscale Model. Simul. **7**, 242 (2008).

[12] B. Voigtlander, T. Weber, P. Smilauer, and D. E. Wolf, Phys. Rev. Lett. **78**, 2164 (1997).

[13] B. S. Swartzentruber, Y.-W. Mo, R. Kariotis, M. G. Lagally, and M. B. Webb, Phys. Rev. Lett. **65**, 1913 (1990).

[14] For $\Delta_+ = 1$, the total number of lateral neighbors is zero before and nonzero after hopping for attachment, or the opposite for detachment.

[15] S. Clarke and D. D. Vvedensky, J. Appl. Phys. **63**, 2272 (1998).

[16] T. Ala-Nissila, R. Ferrando, and S. C. Ying, Adv. Phys. **51**, 949 (2002).

[17] M. Ozdemir and A. Zangwill, Phys. Rev. B **45**, 3718 (1992).

[18] R. Ghez and S. S. Iyer, IBM J. Res. Devel. **32**, 804 (1988)

[19] R. E. Caflisch, M. F. Gyure, B. Merriman, S. J. Osher, C. Ratsch, D. D. Vvedensky, and J. J. Zink, Appl. Math. Lett. **12**, 13 (1999).

[20] C. Ratsch, M. Kang, and R. E. Caflisch, Phys. Rev. E **64**, 020601 (2001).

[21] A. Pimpinelli and J. Villain, *Physics of Crystal Growth* (Cambridge University Press, Cambridge, 1998).

[22] The probability for kink separation na with $a \geqslant 1$ is given by $P(n) = p_k(1-p_k)^{n-1}$, so that $\langle n\rangle = 1/p_k = L_k/a$, and $\langle (n-\langle n\rangle)^2\rangle^{1/2} = (1-p_k)^{1/2}L_k/a \approx L_k/a$ for small $p_k \ll 1$.

[23] Consider choosing a biperiodic kink distribution on both steps where we retain $\{L_{ks+} = 26a, L_{ks-} = 2a\}$ for the smooth step, but replace $L_{kr} = 4$ with $\{L_{kr+} = 5a, L_{kr-} = 3a\}$ or $\{L_{kr+} = 6a, L_{kr-} = 2a\}$ for the rough step. The initial rBCF value for $L_{kr} = 4$ of $R_{vel} = 2.46$ when $W_1 + W_2 = 40a$ changes only slightly to $R_{vel} = 2.44$ or 2.36, respectively.

[24] D. Chadi, Phys. Rev. Lett. **59**, 1691 (1987).

[25] D. Margetis and N. Nakamura, Physica D **240**, 1100 (2011).